TURBULENCE MODELING VALIDATION FOR AFTERBODY FLOWS

A. Hadjadj[1] **and A.N. Kudryavtsev**[2]

[1] LMFN-CORIA, UMR 6614, INSA de Rouen, B.P. 8,
76801 Saint-Etienne du Rouvray, France
[2] Institute of Theoretical and Applied Mechanics,
630090 Novosibirsk, Russia

Introduction

The aerothermodynamics phenomena over space launch vehicles or missiles are a challenging problem on space and aeronautical applications. These physical phenomena can strongly affect the engine's aerodynamic performances. The physical problem met on this geometry is essentially the result of the interaction of two merging flows; one issued from a propulsive jet at high speed and high temperature (flow *2*), and the other (flow *1*) caused by the ambient low speed stream (see Fig. 1).
Several complicating issues are presented in this flow configuration :

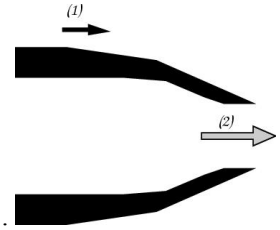

Figure 1. Afterbody nozzle configuration.

- The afterbody flow-field is dominated by the behavior of the turbulent boundary layer. Thus the quality of computational results depends strongly on the accuracy of the turbulence model used for CFD.
- The afterbody configurations are often quite complex, since they include single- or double flux nozzles with a variable geometry, twin-engine with tails and non axisymmetric nozzles with base flows. All of these elements are important, and should be modeled.
- On the other hand, a rather fair prediction of the flow-field can be accompanied by large errors in the calculation of wall properties, affecting mainly transfer coefficients, skin friction and heat flux.

The complexity and the usual misunderstanding of these physical phenomena coupled with the turbulence modeling problem of complex compressible flows motivates the present study. The outline of this paper is as follow: the turbulence models used in this study are given in section 2, the main lines of the numerical method are presented in section 3, the nozzle start-up process is examined in section 4, finally sections 5 and 6 are devoted to the comparisons between numerical and experimental measurements. It is found that an interesting estimation of the pressure coefficient on the afterbody is obtained via the multi-scale model

Turbulence modeling

The oldest and simplest proposal for modeling the turbulent Reynolds stress is Boussinesq isotropic eddy-viscosity concept that assumes an analogy between the viscous stresses in laminar flows and the turbulent stresses in turbulent flows. This concept relates linearly the Reynolds stresses to the mean flow quantities as :

$$\rho \widetilde{u_i'' u_j''} = 2/3\ \rho\, k\, \delta_{ij} - \mu_t \left(S_{ij} - 1/3\ S_{ll}\, \delta_{ij} \right) \qquad (1)$$

where S_{ij} represents the main strain rate and μ_t is the eddy viscosity defined by :

$$\mu_t = C_\mu\, \rho\, k^2 / \varepsilon . \qquad (2)$$

Report Documentation Page

Report Date	Report Type	Dates Covered (from... to)
23 Aug 2002	N/A	-

Title and Subtitle Turbulence Modeling Validation for Afterbody Flows	**Contract Number**
	Grant Number
	Program Element Number
Author(s)	**Project Number**
	Task Number
	Work Unit Number
Performing Organization Name(s) and Address(es) Institute of Theoretical and Applied Mechanics Institutskaya 4/1 Novosibirsk 530090 Russia	**Performing Organization Report Number**
Sponsoring/Monitoring Agency Name(s) and Address(es) EOARD PSC 802 Box 14 FPO 09499-0014	**Sponsor/Monitor's Acronym(s)**
	Sponsor/Monitor's Report Number(s)

Distribution/Availability Statement
Approved for public release, distribution unlimited

Supplementary Notes
See also ADM001433, Conference held International Conference on Methods of Aerophysical Research (11th) Held in Novosibirsk, Russia on 1-7 Jul 2002

Abstract

Subject Terms

Report Classification unclassified	**Classification of this page** unclassified
Classification of Abstract unclassified	**Limitation of Abstract** UU

Number of Pages
6

Equation (2) constitutes a common basis for most turbulence models extensively used today [6]. The baseline model of this study is the standard k–ε model proposed by Jones and Launder [3]. This model based on Boussinesq eddy viscosity concept (relation 2) uses two supplementary equations to describe the whole turbulent flow field.

In this paper, we propose the introduction of several scales characterizing different process of turbulence interaction by using multi-scale model [2], [4], [7]. The multi-scale turbulence modeling consists in partitioning the energy spectrum into several regions, each characterized by a different time scale. Thus different mechanisms such as the return to isotropy, dissipation, diffusion, and viscosity can be modeled using the various characteristic scales. In the simplified split-spectrum used by Kim [4], turbulent transport is described by using two time scales: the first one corresponds to the large eddies and describes generation of turbulent kinetic energy, and the second one corresponds to the smaller-scale eddies and describes dissipation rate. The turbulent energy can be partitioned into three regions: production region, characterized by the turbulent kinetic energy k_p and the energy transfer rate ε_p, transfer region, characterized by the turbulent kinetic energy k_t and the dissipation rate ε_t and dissipation region, where the turbulent kinetic energy is dissipated into heat.

This model employs four supplementary transport equations to described large and small eddies motion (for more details see Kim [4]). One of the most interest of the multi-scale model is the expression of the eddy viscosity, given by:

$$\mu_t = C_\mu \rho k^2 / \varepsilon_p . \tag{3}$$

where $k = k_p + k_t$. By rearranging the equation (3), we obtain :

$$\mu_t = C_\mu (\varepsilon_t/\varepsilon_p) \rho k^2 / \varepsilon_t = F(\varepsilon_t/\varepsilon_p) \rho k^2 / \varepsilon . \tag{4}$$

Note that, in the proposed multi-scale model, C_μ becomes function of $\varepsilon_t/\varepsilon_p$. Therefore, for turbulence equilibrium conditions, this function F is equal to a constant value in the classical k-ε model. In this case, the multi-scale turbulence model becomes a single scale turbulence model. In the case of non equilibrium turbulent flow, for example when the energy transfer rate from large eddies is more important than the dissipation rate at small eddies, the eddy viscosity μ_t decreases, which implies a decreasing of the turbulent kinetic production. Inversely, this term permits to increase the turbulent kinetic production. The multi-scale spectral decomposition yields to a variable C_μ which accounts for turbulence non equilibrium effects.

Computational results

Afterbody mesh grid. The computational domain is splitted into two connected sub-domains (see Fig. 2) : the first one includes the nozzle with a propulsive jet, and the second one concerns the ambient low speed flow. The downstream region of the nozzle has been described

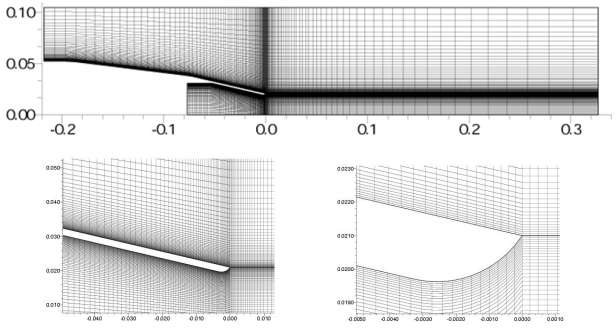

Figure 2. Computational domain (Grid detail near trailing edge).

in detail with a sufficient number of points in order to solve correctly the throat region where sonic speed is attained. Additional mesh grid refinement was provided near the trailing edge of the nozzle so as to predict as well as possible the entrainment effect issued from boundary layers evolution, into the free shear layer between the plume and the free stream flow. The computational domain is discretized into a 330×150 mesh with a concentration of grid points near afterbody walls. The mesh size of the first grid point from the wall is located at $y^+ \approx 1$. Extensive grid refinement tests were achieved to insure that the results are mesh independent.

Numerical aspects. The Reynolds-averaged Navier – Stokes equations associated with a turbulence model are solved on a computational domain of variables ξ and η (transformed coordinates of the physical domain), by the use of finite volumes discretization technique on structured mesh. The new system of equations is solved by using an explicit-implicit scheme which is second-order accurate in space and time (see Vandromme *et al.* [8], [9]). The basic discretization for the convective fluxes is modified so as to take into account the physical properties of information propagation. The viscous terms are centered and the axisymmetric source terms are integrated at the center of each control volume in both the ξ and η directional sweeps.

To reach a steady-state solution with a minimum number of iterations, the explicit discretization is complemented with an implicit numerical approximation which is free from stability conditions. Thus, the block pentadiagonal system is solved by generalized Thomas algorithm with *LU* decomposition in the η direction, and by a line Gauss–Seidel relaxation technique in the ξ direction. As the system is really diagonally dominant and the method is iterative, converged steady solution can be obtained in very limited number of time steps, each time step including a double sweep (backward-forward) in the flow direction. With this technique, unbounded time step values can be used. Numerical simulations have been made with C.F.L. numbers greater than 10^4.

The numerical boundary conditions used in this work are far-field non-reflecting boundary conditions for ambient low speed stream, adiabatic no-slip wall and symmetry boundary condition. At the inlet, the profiles of all quantities are imposed; including total pressure and temperature P_t, T_t, turbulent kinetic energy k and dissipation rate ε. Theses profiles are based on the computational results of the fully developed boundary layer flow.

Axisymmetric afterbody flow (hot jet). In this study, we are interested in the S3Ch single-flux axisymmetric nozzle [1], [10], for which detailed measurements are available. This test case permits an accurate validation of turbulence models using CFD. The nominal flow conditions are :

- **Outer flow**

– upstream Mach number $M_\infty = 0.8$

– stagnation pressure : $P_t = 10^5$ Pa

– stagnation temperature : $T_t = 300$ K

– incident boundary layer thickness ($\delta \approx 8$ mm)

- **Jet flow**

– stagnation pressure : $P_t = 3.15\ 10^5$ Pa

– stagnation temperature : $T_t = 900$ K

– jet expansion ratio : $P_t/P_a = 4.80$

In order to analyze the basic characters of the physical phenomenon, both steady and unsteady calculations for inviscid and viscous flow have been performed.

Nozzle start-up process

Firstly, it is interesting to analyze, via numerical simulation, the nozzle start-up process. This simulation starts when the diaphragm, located at the inlet nozzle, is removed till the establishment of the propulsive jet far field downstream of the nozzle. The calculation is performed by solving Euler equations, since the inviscid effect (waves propagation and vortex formation) plays a major role during this phase.

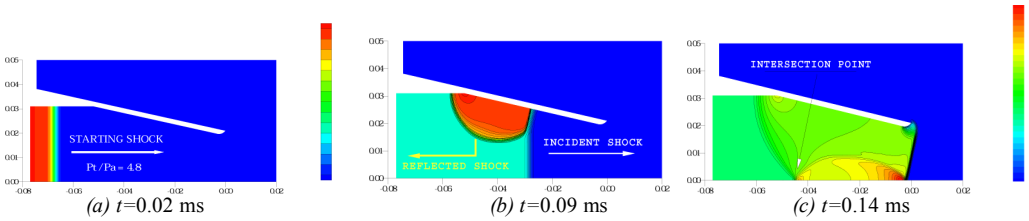

(a) t=0.02 ms *(b)* t=0.09 ms *(c)* t=0.14 ms

Figure 3. Pressure field (min = 0.65, max = 3.70) bar.

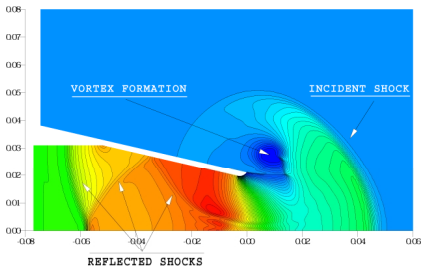

Figure 4. Pressure field at t = 0.20 ms (min = 0.10, max = 3.59) bar

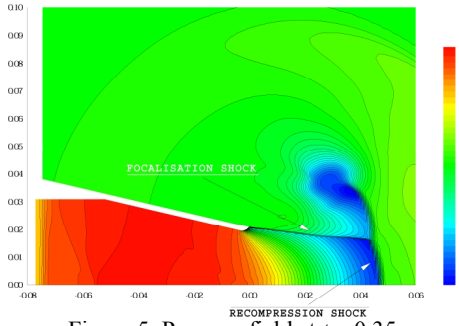

Figure 5. Pressure field at t = 0.35 ms (min = 0.09, max = 4.21) bar

As mentioned above, the computation starts impulsively, and the pressure ratio is assigned to be 4.80. Several time sequences of color pictures (pressure field) are presented in Figs. 3-5 to illustrate the shock waves propagation. Figure 3.*a* depicts the starting shock pulsed within the nozzle. Under a high pressure gradient effect, and due to nozzle geometry (convergent part) the incident shock interacts with the wall and creates a series of complicated waves ; A reflected shock propagates upstream of the nozzle, a quasi-normal shock near the wall and a slip line emanates from the triple point (see Fig. 3.*b*).

The new shock configuration interacts with the axis and generates a complex network of waves (see Figs. 3.*c* and 4). At the nozzle exit, the flow is highly under-expanded, and consequently, a low density vortex core is generated (see Fig. 4). The reversed flow is afterwards convected downstream during the starting process. Upstream of the incident shock, the flow is highly decelerated and the static pressure is nearly equal to the stagnation pressure. In the supersonic jet, a double compression process is achieved through a straight longitudinal Mach disc and a curved transversal shock. At this time, we observe once again a brief apparition of the triple point configuration (see Fig. 5). In fact, this flow configuration is unstable. Thus, at t = 0.3 ms, the Mach disc disappears and the oblique shock deviates towards the axis. The inclination of the stream causes the shock wave to be deflected and meet the axis at a single point.

Finally, two different streams are formed; the first one represents the propulsive jet with downstream alternatives expansion and compression regions and the second one constitutes the uniform subsonic flow.

In the following sections, we focus our study on the turbulence modeling, our main objective is to seek out the possibilities of using the multi-scale turbulence model to reproduce the major features of nozzle afterbody flows.

Flow feature description

For a laminar flow, the velocity field shows a separated boundary layer along the nozzle shoulder. This result is illustrated by the velocity vector field near the nozzle trailing edge (see

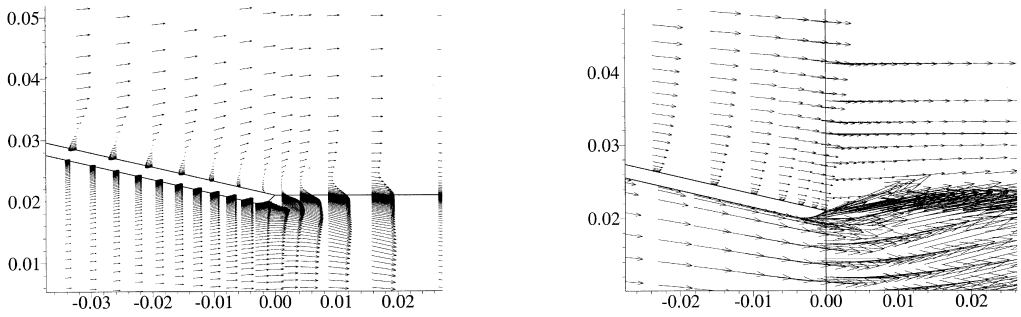

(a) laminar flow (b) *turbulent flow*

Figure 6. Velocity vector on the afterbody/

Fig. 6. *a*). The boundary layer separation phenomenon has been already observed in many calculations mainly those done by SNECMA and Mc Donnell Douglas [10], [1]. However, this result do not reflect reality. Indeed, the experimental boundary layer velocity profiles indicate that there is no separation along the nozzle shoulder [1].

The obtained results, even if they are in contradiction with the experimental data, can be easily explained by the boundary layer effects. It is clear that the laminar boundary layer profile developed along the nozzle shape is less energetic and consequently less resistant to the adverse pressure gradient, which causes its separation from the wall. For turbulent flow, the computational result shows that there is no boundary layer separation on the afterbody (see Fig. 6. *b*). This result is in good agreement with experimental data.

Aerodynamics of afterbody

One important characteristic of predicting afterbody flows, lies in the fact that the surface pressure distribution may significantly affect the engine's aerodynamics performances. So, it is necessary to accurately predict the pressure on the afterbody. Therefore, the pressure coefficient C_p is given by :

$$C_p = 0.5\,(p - p_\infty) / \rho_\infty U^2_\infty \qquad (5)$$

where the subscript "∞" refers to the upstream flow conditions. The experimental afterbody model is equipped with a total of 48 pressure orifices located along the nozzle contour. The nozzle and the afterbody are defined in Fig. 2. The geometry contour of the afterbody is made of rectilinear segments, the shape consisting of two successive conical surfaces with an angle 7° and 13°, respectively. The total length of the afterbody is 218 mm.

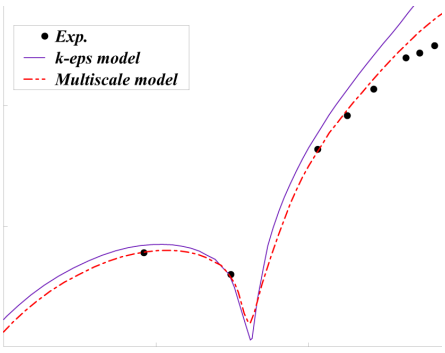

Figure 7. Static pressure coefficient on the afterbody

Approaching the afterbody and nozzle, the boundary layer is growing slowly in a near constant pressure. The shoulder at the beginning of the nozzle creates a locally minimum pressure. Past this minimum point, the gradient becomes adverse and the boundary layer begins thickening rapidly. This adverse pressure gradient still acts until reaching the nozzle exit. The interaction in the final adverse pressure gradient region is recognized as the key problem in predicting

Figure 7 shows the calculated and the measured wall pressure coefficient C_p on the afterbody. From a

general point of view, the two simulations presented herein (k–ε and multi-scale models), give more or less the same trend: a rather good prediction of the pressure distribution in the upstream part of the afterbody. However, at the end of the shoulder, the k–ε model shows an important discrepancy with the experimental data. The C_p is overestimated of almost 30 %, which is unacceptable from aerodynamics point of view. This result shows one of the weakness of the k–ε model, to reproduce the entrainment effect of boundary layer flow at the end of the body. It should be pointed out that without an accurate prediction of the pressure distribution in this region, any drag estimation is meaningless. Therefore, the obtained results with the multi-scale model are significantly in better agreement with the experimental data. This model reproduces correctly the flow behavior in this region; the physical processes of boundary layer expansion and compression is quite well described, and the difference observed at the nozzle trailing edge is reduced to 10 %.

At this stage, it would be important to know that the upstream boundary condition have a great influence on the pressure distribution on the afterbody. The upstream boundary of the computational domain is located in the cylindrical section of the afterbody model. The only experimental data available in this region is a pitot pressure profile. Without any further information about the temperature and turbulent quantities profiles in the incoming boundary layer, some assumptions should be made to evaluate the missing quantities. The computations done by SNECMA [5] show that the variation of the incident boundary layer modifies significantly the pressure value at the nozzle trailing edge. For example, a boundary layer with a thickness δ = 1.5 cm gives a result closer to experimental point than one with a thickness δ = 0.8 cm. In this study, our strategy of investigation is to keep constant the incident boundary layer thickness δ and to improve the accuracy of turbulence modeling.

Conclusion

In this study, a multiple-time-scale model was investigated. The basic form of model equations were introduced and applied to an afterbody nozzle flow with a propulsive jet. It was shown that the present model can satisfactorily reproduce the physical phenomena encountered in this geometry. The upstream conditions even if difficult to determine, have to be considered with accuracy. This particular point makes the computation even more difficult because the steady state depends strongly on the slightest variation of the subsonic boundary condition. Convergent-divergent axisymmetric exhaust nozzles may present considerable loss of thrust if they operate under highly over-expansion regime. Thus different nozzle shapes like double-flux geometry will be a topic of further works.

REFERENCES

1. **Bailly D., Regard D., Pillon J. A.** Essai de la tuyère de référence dans une soufflerie S3Ch et première qualifications de la tuyère ventilée. Rapport de Synthèse Final N0 42/3482 AY, ONERA, 1991.
2. **Hadjadj A., Vandromme D., De Chantérac L.** Computations of compressible turbulent shear flows with multiple-time-scale models. In: Proceedings of the 11th T.S.F. Symp., 1997, Vol. 3, pp. 32.
3. **Jones W. P., Launder B. E.** The calculation of low-Reynolds-number phenomena with a two-equation model of turbulence. Journal of Heat and Mass Transfer, 1973. Vol. 16, pp. 1119-1130,
4. **Kim S.W.** Calculations of divergent channels flows with a multiple-time-scale turbulence model. AIAA J. 1991. Vol. 29, No. 4.
5. **Moreau S., Mauffret T.** Numerical simulations of afterbody flow-fields with two-equation turbulence models. AIAA 96-0570, 1996.
6. **Patel V. C., Rodi W., Scheuerer G.** Turbulence models for near-wall and low Reynolds number flows: A review, AIAA J., 1985, Vol. 23.
7. **Schiestel R.**, Multiple-time-scale modelling of turbulent flows in one point closures, Phys. Fluids 1987, 30 (3),
8. **Vandromme D., HaMinh H., Viegas J.R., Rubesin R.W., Kollman W.** Second order clossure for the calculation of compressible wall bounded flows with an implicit Navier–Stokes solver. In: Proc. of the 4th T.S.F. Symp., Karlsrube, 1983.
9. **Vandromme D., Saouab A.** Implicit Solution of Reynolds-Averaged Navier-Stokes Equations for Supersonic Jets on Adaptative Mesh. In: Proc. of the 1st European Computational Fluid Dynamics Conf., Belgium, 1992.
10. **AR-318** AGARD Working Group on Aerodynamics of 3-D Aircraft After-bodies, AGARD Advisory Report, N°318, 1995.